

Changes to the HIRLAM needed for finer grids?

A McDonald, Met Éireann. Dublin, Ireland.

1. Background.

DNMI have been experiencing problems using the semi-Lagrangian scheme on a $0.1^\circ \times 0.1^\circ \times 31$ grid with a 240s time step. They have reported large vertical velocities over the Norwegian mountains and also occasional ‘crashes’. In particular, they made available a data set starting from 2000/02/04 which ‘crashed’ at time step 142 (approximately 9.5h) with an unphysical maximum wind speed of 323m/s at grid point (148,139,11), which is over Southern Norway. In this note this data set is used to probe some weaknesses in the HIRLAM reference system and to suggest some improvements.

2. Process splitting versus fractional stepping.

There is an accumulation of evidence that for the vertical diffusion scheme fractional stepping is more stable than process splitting. See, for example, McDonald (1996), Jones (2001), Tijm (2002). Therefore an obvious first test was to re-run the above-mentioned forecast with the parameter ‘nldynvd’ set ‘TRUE’. This causes the vertical diffusion scheme to use the fields which have been updated by the dynamics. This eliminated the ‘crash’. The model completed a 24h forecast (not shown) with no sign of instability.

3. Smoother discretization of the temperature equation.

Although switching to fractional stepping eliminated the ‘crash’ there remained some aspects of the forecast which gave cause for concern. One of these is illustrated in Fig. 1, which shows an unphysical temperature of 113°C at level 31 in the vicinity of Jan Mayen Island. This is a 6h forecast generated using no physics to emphasise that the problem originates in the dynamics. Also, a time step of 900s and no horizontal diffusion were used in order to exaggerate the forecast error. (A time step of 900s is typically 15 times as large as the maximum allowable Eulerian time step.) We will call this experiment 1 for discussion purposes below. This error was eliminated as follows by using an idea of Ritchie and Tanguay (1996).

The temperature equation can be written as, using the notation of the HIRLAM documentation manual, and ignoring the physics and diffusion terms,

$$\frac{dT_k}{dt_k} = \left[\frac{\kappa T_v}{1 + (\delta - 1)q} \right]_k \left(\frac{\omega}{p} \right)_k. \quad (3.1)$$

Defining T_b as (see section 2.1.4 of the HIRLAM documentation manual)

$$T_b = - \left(p_s \frac{\partial p}{\partial p_s} \frac{\partial T}{\partial p} \right)_{ref} \frac{\Phi_s}{R_d T^r} \quad (3.2)$$

and defining $T = T' + T_b$ we can re-write Eq. (3.1) as

$$\frac{dT'_k}{dt_k} = \left[\frac{\kappa T_v}{1 + (\delta - 1)q} \right]_k \left(\frac{\omega}{p} \right)_k - \mathbf{v}_H \cdot \nabla T_b - \dot{\eta} \frac{\partial T_b}{\partial \eta}. \quad (3.3)$$

We now use the traditional semi-Lagrangian discretization except that we discretize the advection terms on the right hand side of Eq. (3.3) in an Eulerian fashion and include them in the non-linear terms:

$$(T')_k^{n+1} + \frac{\Delta t_+}{2}(\tau \cdot \mathbf{D})_k^{n+1} = \left[(T')^n - \frac{\Delta t_-}{2}\tau \cdot \mathbf{D}^n + \frac{\Delta t_-}{2}(N_T)^{n+1/2} \right]_{k,*} + \frac{\Delta t_+}{2}(N_T)_k^{n+1/2}, \quad (3.4)$$

where, as usual,

$$(\tau \cdot \mathbf{D})_k = \kappa T^r \left\{ \left(\frac{\Delta \ln p}{\Delta p} \right)_k^r \sum_{j=1}^{k-1} D_j \Delta p_j^r + \alpha_k^r D_k \right\} \quad (3.5)$$

but now

$$(N_T) = \tau \cdot \mathbf{D} + \frac{\kappa T_v}{1 + (\delta - 1)q} \left(\frac{\omega}{p} \right) - \mathbf{v}_H \cdot \nabla T_b - \dot{\eta} \frac{\partial T_b}{\partial \eta}. \quad (3.6)$$

From Eq. (3.4) we see that formally the discretization is unchanged. We simply have a new definition of N_T given by Eq. (3.6).

When we use this treatment of the temperature equation the behaviour of the level 31 temperature in the vicinity of Jan Mayen Island is much more realistic when we repeat experiment 1; see Fig. 2. There is a volcano in the north of the Island of altitude 2277m; so the temperature of -17°C is not unreasonable. We will call this experiment 2 for discussion purposes below.

4. Extrapolation along the trajectory.

We might expect a general reduction of noise in the vicinity of steep orography to come from this change to the treatment of the temperature. A convenient crude measure of noise is the square root of the vertical velocity at 300hPa summed in the horizontal over all of the grid points and divided by N , the total number of grid points: $\langle \omega \rangle = \{\sum_{i,j} \omega_{i,j}^2\}^{1/2}/N$. In table 1 we display the maximum, minimum, and rms values of ω at 300hPa for experiments 1 and 2. As we can see there has been a significant reduction in noise, which is confirmed by comparing Figs. 3 and 4. Notice the improvement over Iceland and Norway. However, all is not well. There is residual noise over the ocean. What can we do about that?

Experiment	ω_{min}	ω_{max}	$\langle \omega \rangle$
1	-8.26	7.80	0.59
2	-4.98	7.66	0.48
3	-5.13	3.79	0.31
4	-6.02	5.79	0.33
5	-4.77	3.83	0.30

TABLE 1. Minimum, maximum and root mean square ω at 300hPa in units of Pa/s.

In McDonald (1999a) various methods for finding the departure point position were tested. The method which gave the smallest amount of noise, as measured by the smallest value of $\langle \omega \rangle$ ($= 0.129$) was subsequently installed in the HIRLAM reference system. The tests in that paper were performed on a $0.3^\circ \times 0.3^\circ \times 24$ grid using a 900s time step. As was discussed in section 4 of that paper ‘extrapolation along the trajectory’ has the attractive theoretical feature that its stability is independent of the number of grid points between the arrival and departure points. However, it gave $\langle \omega \rangle = 0.138$, and was, by implication, more noisy. The Hortal (1998) scheme gave $\langle \omega \rangle = 0.162$ and was visibly noisier in those tests.

Let us re-visit these methods for computing the departure point position now that we have another forecast containing significant noise, and a much finer grid, by repeating experiment 2, but with alternative computations of the departure point position. Therefore, for experiment 3 we are using no physics, no diffusion, $\Delta t = 900\text{s}$, the new treatment of temperature, and ‘extrapolation along the trajectory’. The resulting 6h forecast of 300hPa vertical velocity shows a significant reduction in noise over the ocean, North Sea, Scotland and southern Sweden; see Fig. 5. This is confirmed by table 1, which shows $\langle \omega \rangle = 0.31$, in contrast to $\langle \omega \rangle = 0.48$ for experiment 2. Repeating this experiment using the ‘Hortal scheme’ (experiment 4), we can conclude from table 1 and Fig. 6 that this is almost, but not quite, as good as ‘extrapolation along the trajectory’.

5. Smoother interpolation.

The vertical velocity $\dot{\eta}$ is defined on the half levels. For the semi-Lagrangian integration we need it at the full levels. In the reference system we use a cubic interpolation to do this. This can make an already noisy field even noisier. Thus in the ECMWF model they use a linear interpolation; see Eq. (3.6) of White (2000). Repeating experiment 3 with this change also shows a small positive impact; see Table 1, where we call this experiment 5.

6. Filtering the orography.

Do these changes have any impact when the physics is switched back on? Using HIRLAM5.0 plus the changes described in sections 2-5 and a time step of 240s (experiment 6) the rainfall over the southern Norwegian mountains still looks suspect; see Fig. 9. The large values at single grid points are almost certainly unphysical. Thus, there continues to be a problem over steep orography. Repeating this forecast with a 60s time gives almost the same forecast (not shown). Since for such a small time step $u\Delta t/\Delta x < 1$ this is not an ‘orographic resonance’ problem. (With such a time step the semi-Lagrangian scheme can be thought of as a modified Lax Wendroff discretization scheme). To find an explanation let us look again at filtering the orography; see McDonald and de Bruijn (1998) and McDonald (1999b).

The two-grid-wave group velocity is hopelessly inaccurate for both the semi-Lagrangian and Eulerian discretization of the advection equation. Consider the one dimensional advection equation,

$$\frac{\partial\psi(x,t)}{\partial t} + u_0\frac{\partial\psi(x,t)}{\partial x} = 0. \quad (6.1)$$

Using the semi-Lagrangian discretization with a cubic interpolation the group velocity is given by Eq. (4.9) of McDonald (1999b); it is displayed in Fig. 7. Using a leapfrog discretization results in the group velocity given by the formula on page 117 of Haltiner and Williams (1980). It is displayed in Fig. 8. Notice that for waves larger than approximately four grids ($k\Delta x = \pi/2$) the semi-Lagrangian scheme is more accurate than the leapfrog scheme. However for two grid waves ($k\Delta x = \pi$) it behaves appallingly, varying between $-1.66u_0$ for $\alpha = 0$ and $-\infty$ for $\alpha = 0.5-$, and between $+\infty$ for $\alpha = 0.5+$ and u_0 for $\alpha = 1$; ($\alpha = u_0\Delta t/\Delta x$). Since the amplitude of the two-grid wave with $\alpha = 0.5$ is zero these infinite values are not catastrophic. (Because the denominator in Eq. (4.9) of McDonald (1999b) is the amplitude squared, the amplitude will always be small when the group velocity is large). The leapfrog scheme is not so badly behaved for two-grid waves: $u_g(2\Delta x) = -u_0$.

As long as the amplitude of the two-grid wave remains small these inaccurate group velocities need not concern us. By definition we are trying to model much longer-wave phenomena. However, if their amplitude grows, large amplitude two-grid waves will be advected totally inaccurately by the advection scheme; this is just noise, by definition. Let us postulate that this is the source of the ‘grid point storms’ seen in Fig. 9.

Looking at Fig. 7, we could argue that we should filter all structure of four grids ($k\Delta x = \pi/2$) or less from the orography. With the filter I am using (the Raymond, 1988, filter) such a sharp cut-off is not possible. See Fig. 1 of McDonald and de Bruijn (1998), where the response function is displayed. As a compromise I have chosen $\epsilon = 0.1$, which as can be seen from that figure reduces the amplitude (normalized to 1) of the three-grid and four-grid waves to about 0.25 and 0.9, respectively, while eliminating the two-grid wave entirely. With the new orography were the ‘grid point storms’ eliminated? Yes; repeating experiment 6 with the orography thus filtered yields the rainfall forecast shown in Fig. 10. The ‘grid point storms’ have been eliminated.

7. Discussion.

Fractional stepping for the vertical diffusion scheme has been shown to give more stable forecasts. Also, the new treatment of the temperature equation, ‘extrapolation along the trajectory, and to a lesser extent, linear interpolation to compute $\dot{\eta}$ at the full levels all act to reduce noise in the integration when we used no physics, no diffusion, and a very large time step. However, all of these in combination have little impact on the ‘grid point storms’ seen in the rainfall charts. To eliminate them it is necessary to

filter the orography. It would be nice to find a filter with a sharper cut-off close to four grids than the Raymond (1988) filter.

Acknowledgment. Thanks to Ray McGrath for supplying a script for filtering the orography of the initial and boundary files. Also, thanks to Jim Hamilton for assistance with the graphics.

References.

- Haltiner, G.J., and R.T. Williams, 1980: *Numerical prediction and dynamic meteorology*. Wiley.
- Hortal, M., 1998: Some recent advances at ECMWF. *LAM Newsletter* **27** 32-36. Available from M. Hortal, ECMWF, Reading RG2 9AX, England.
- Jones, C., 2001: A brief description of RCA2 (Rossby centre atmosphere model, version 2) *SWE-CLIM newsletter* **11**, 9-14.
- McDonald, A., 1996: Noise caused by updating the 'physics' with large time steps. *HIRLAM newsletter* **25**, 15-20.
- McDonald, A., and Cisco de Bruijn 1998: Impact of filtering the HIRLAM orography. *HIRLAM newsletter* **30**, 43-46.
- McDonald, A., 1999a: An examination of alternative extrapolations to find the departure point position in a 'two time level' semi-Lagrangian integration. *Mon. Wea. Rev.* **127**, 1985-1993.
- McDonald, A., 1999b: The origin of noise in semi-Lagrangian integrations. *Seminar proceedings on Recent Developments in Numerical Methods for Atmospheric Modelling; 7-11 September, 1998*. 308-335. Available from the European Center for Medium range Weather Forecasting, Reading, England.
- Raymond, W.H., 1988: High-order low-pass implicit tangent filters for use in finite area calculations. *Mon. Wea. Rev.*, **116**, 2132-2141.
- Ritchie, H., and M. Tanguay, 1996: A comparison of spatially averaged Eulerian and semi-Lagrangian treatments of mountains. *Mon. Wea. Rev.*, **124**, 167-181.
- Tijm, S., 2002: Waves in the wind. <http://www.knmi.nl/~tijm/waves.html>
- White, P.W., 2000: IFS Documentation part III: dynamics and numerical procedures (CY21R4). Available from ECMWF, Shinfield Park, Reading, England.

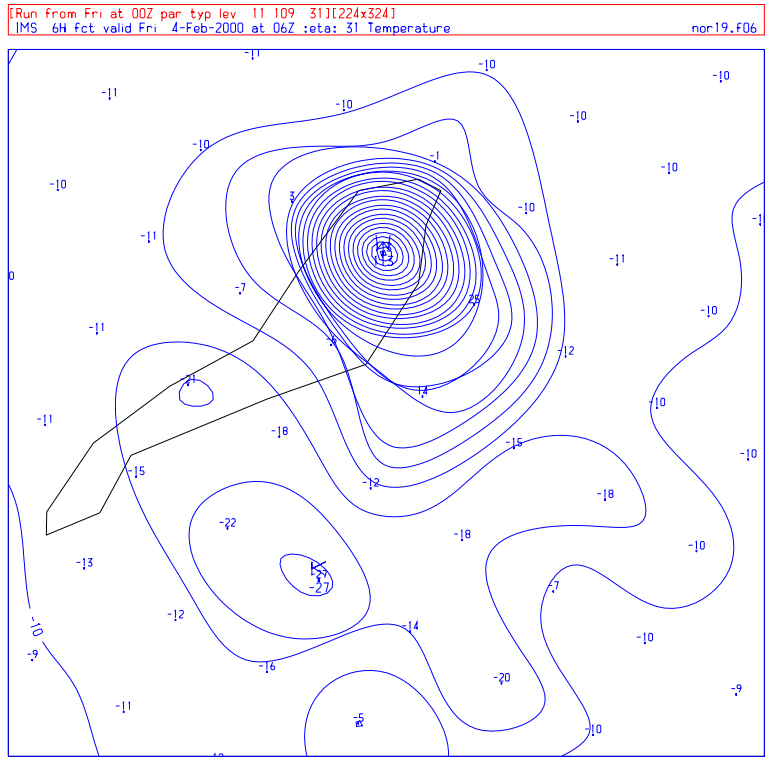


Figure 1: 6h forecast of the temperature at level 31 using no physics and no diffusion. The contours are every 5°C

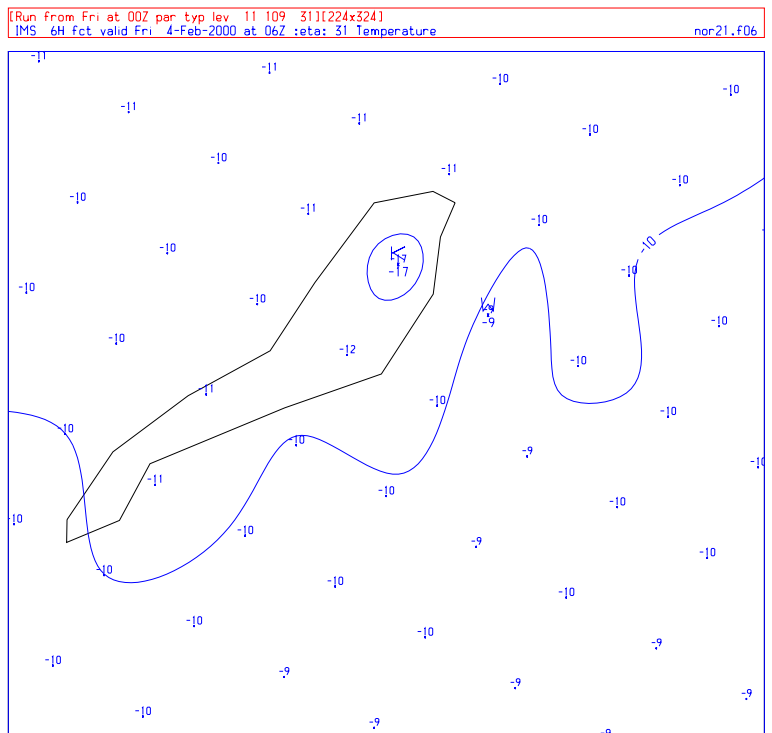


Figure 2: Same as Fig. 1, but now replacing the HIRLAM5.0 reference treatment of the temperature equation with Eqs. (3.4)-(3.6).

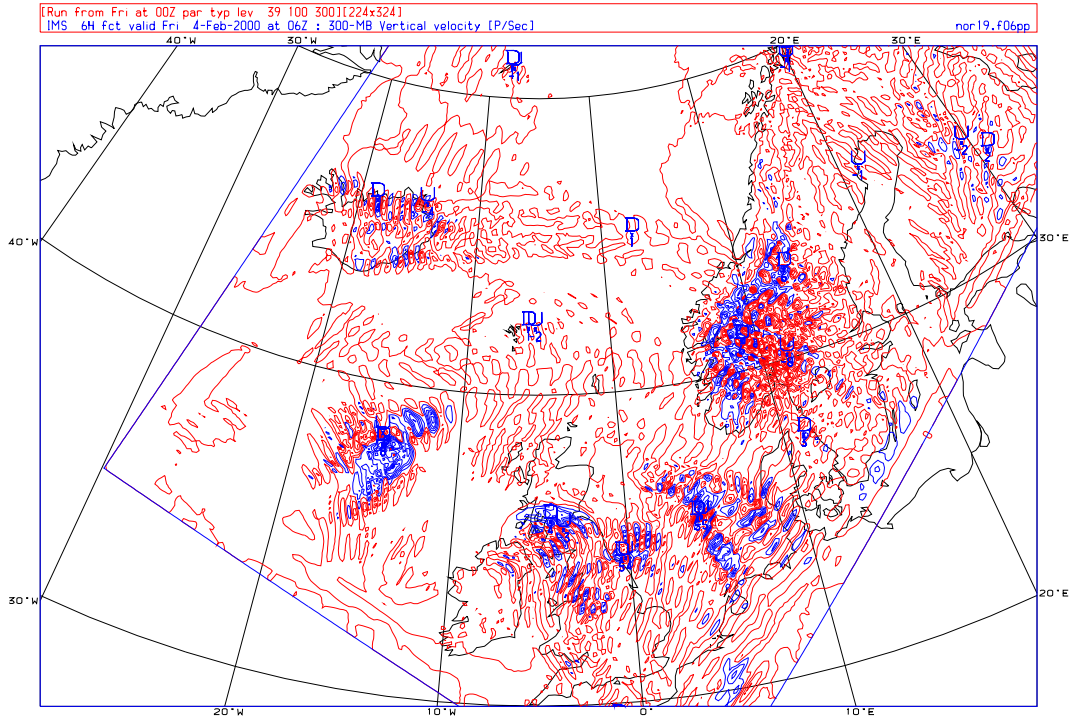


Figure 3: 6h forecast of the 300hPa vertical velocity in Pa/s using no physics and no diffusion. The contours are every hPa

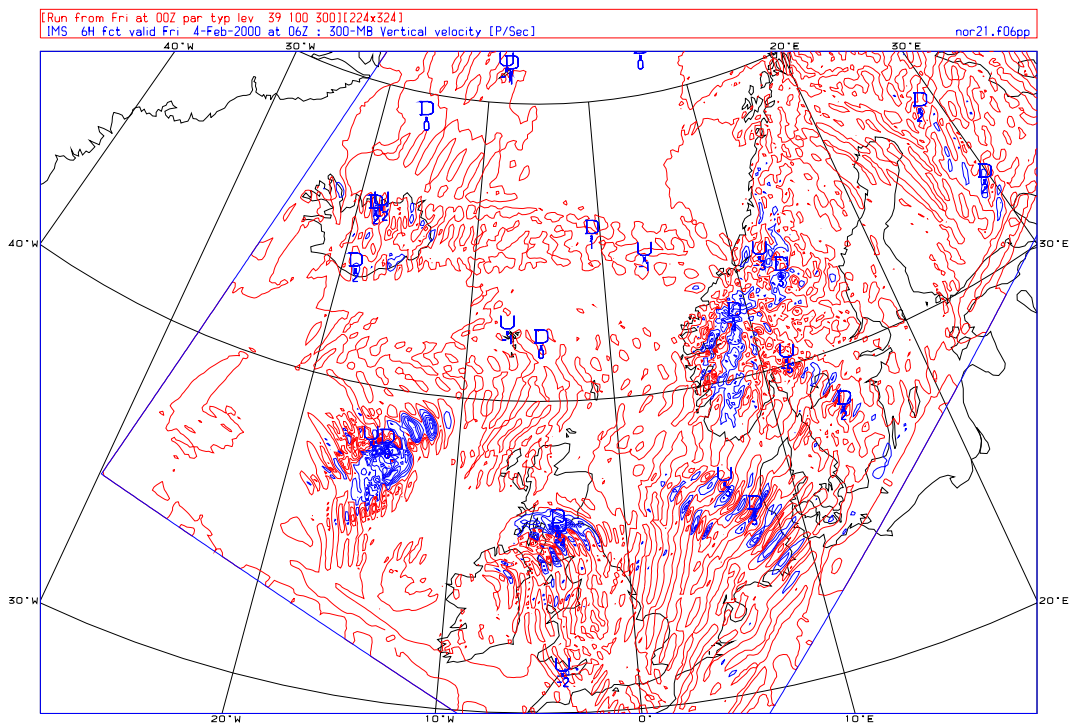


Figure 4: Same as Fig. 3, but now using Eqs. (3.4)-(3.6) in place of the reference treatment of the temperature equation.

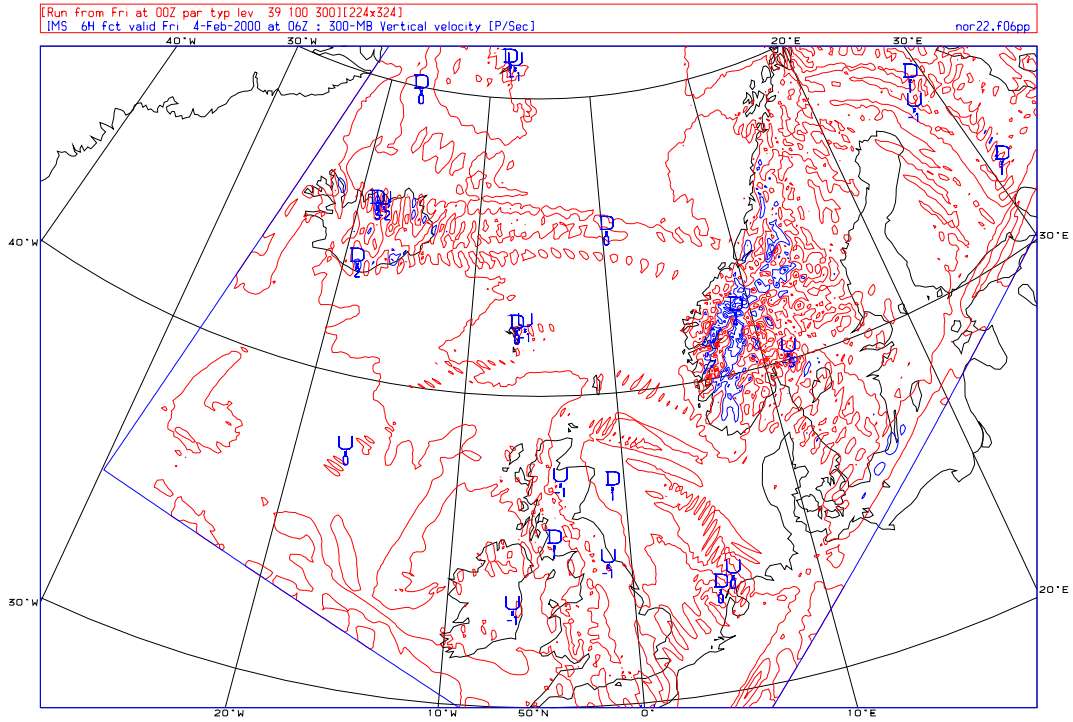


Figure 5: Same as Fig. 3, but now using Eqs. (3.4)-(3.6) in place of the reference treatment of the temperature equation and also using 'extrapolation along the trajectory' to compute the departure point position.

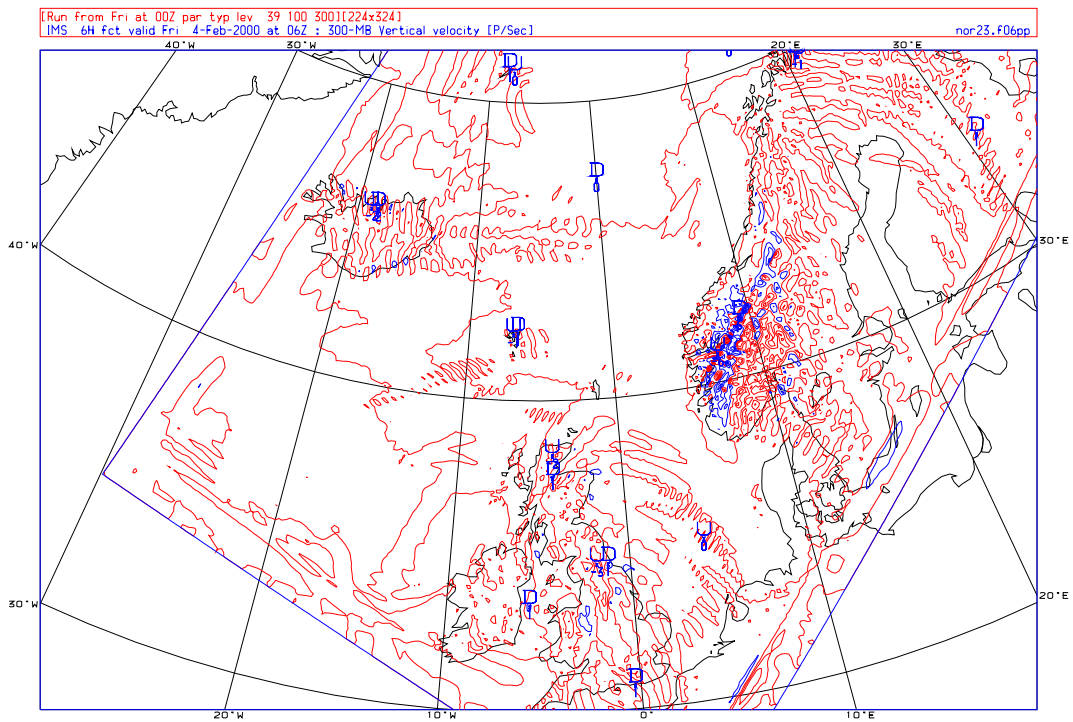


Figure 6: Same as Fig. 3, but now using Eqs. (3.4)-(3.6) in place of the reference treatment of the temperature equation and also using 'the Hortal scheme' to compute the departure point position.

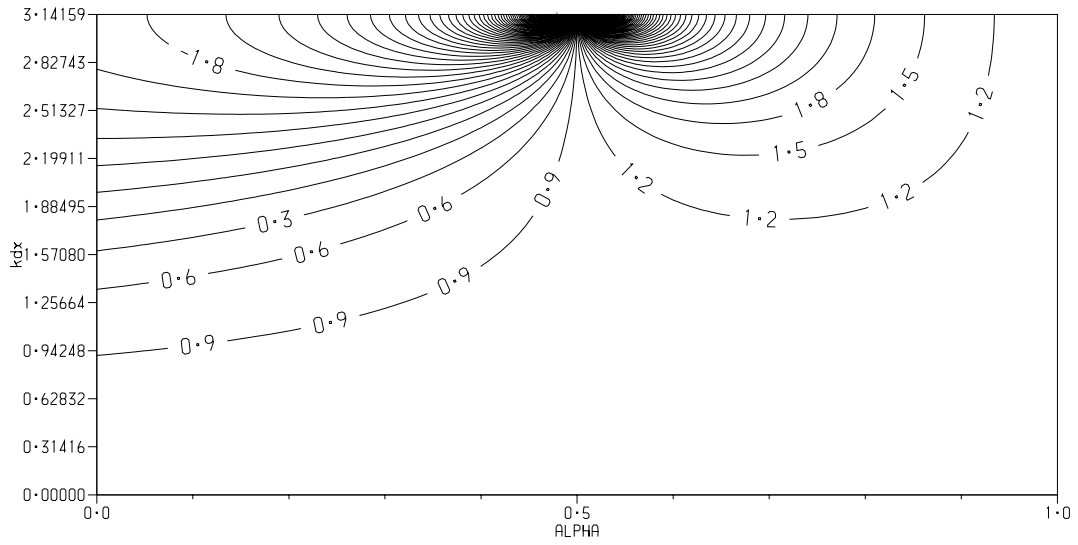


Figure 7: Group velocity normalised to u_0 associated with the semi-Lagrangian discretization of Eq. (6.1). On the x-axis is $\alpha = u_0 \Delta t / \Delta x$, and on the y-axis is Δx times the wave number, which varies from 0 to π .

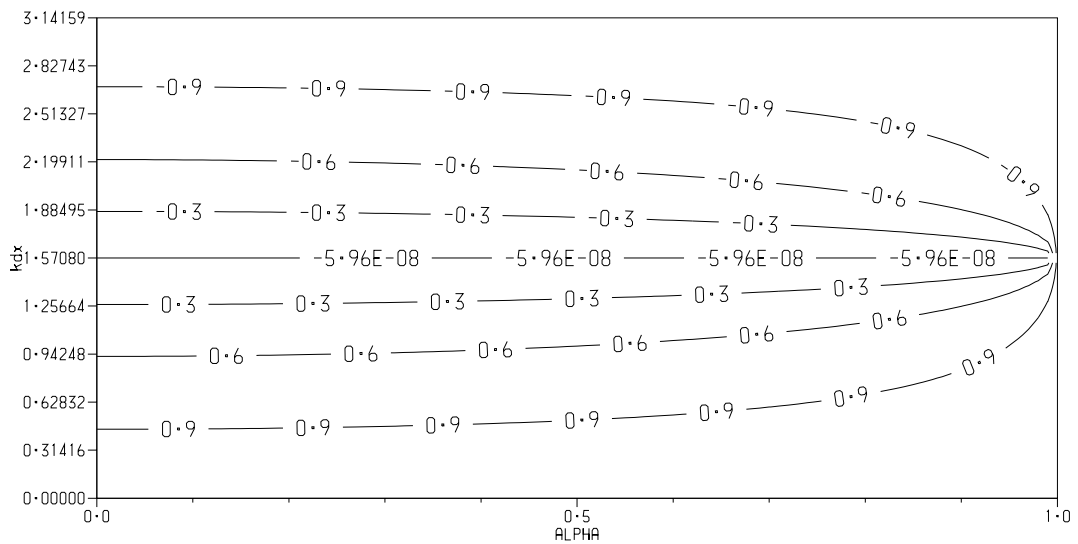


Figure 8: Same as Fig. 7, but now using the leapfrog discretization.

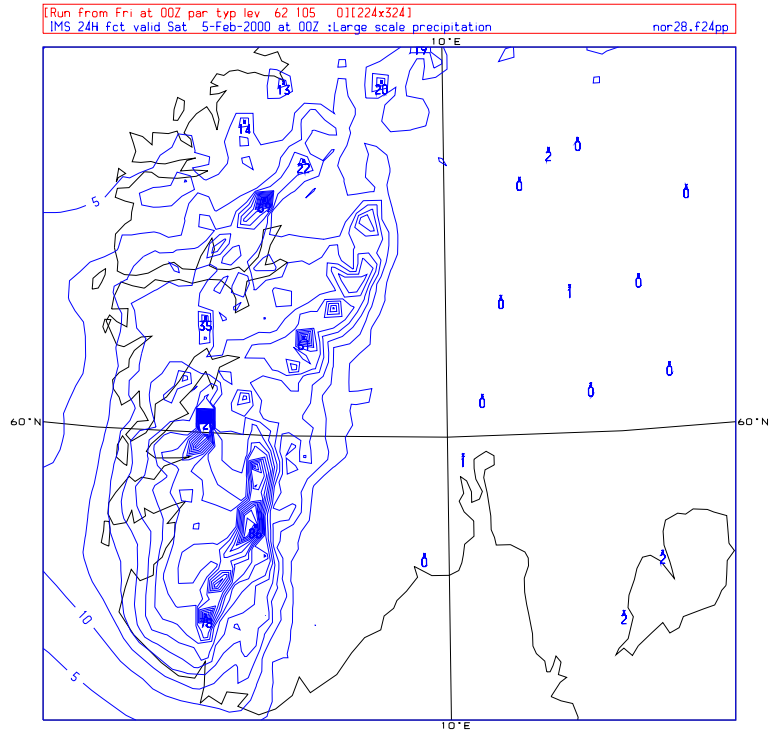


Figure 9: 24h forecast of the large scale rainfall over southern Norway and south-western Sweden using HIRLAM5.0 plus the updates described in sections 2-5;

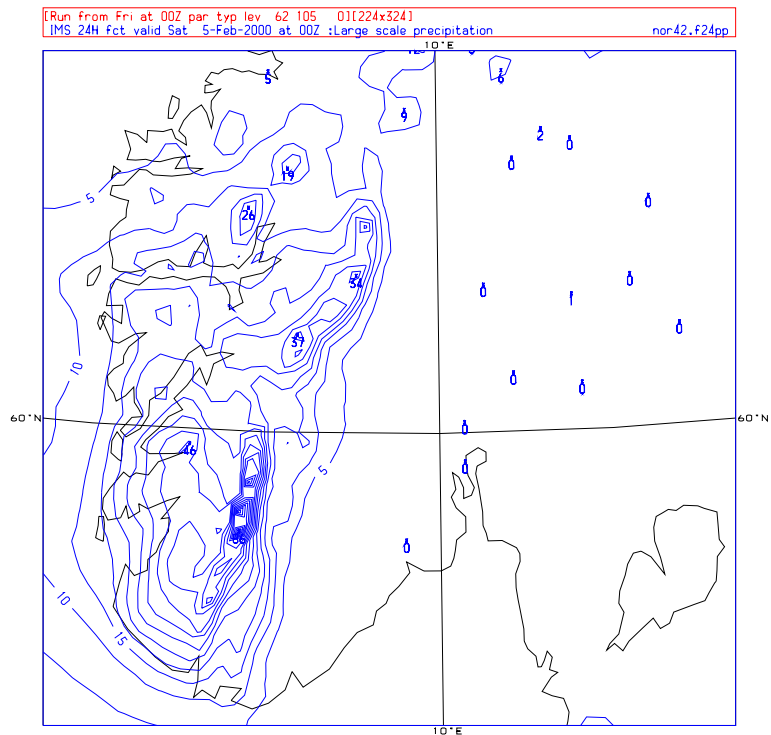


Figure 10: Same as Fig. 9, but now using filtered orography instead of the reference orography.